



Lawrence Berkeley National Laboratory

Quayside Energy Systems Analysis

Michael Wetter
Jianjun Hu

Lawrence Berkeley National Laboratory

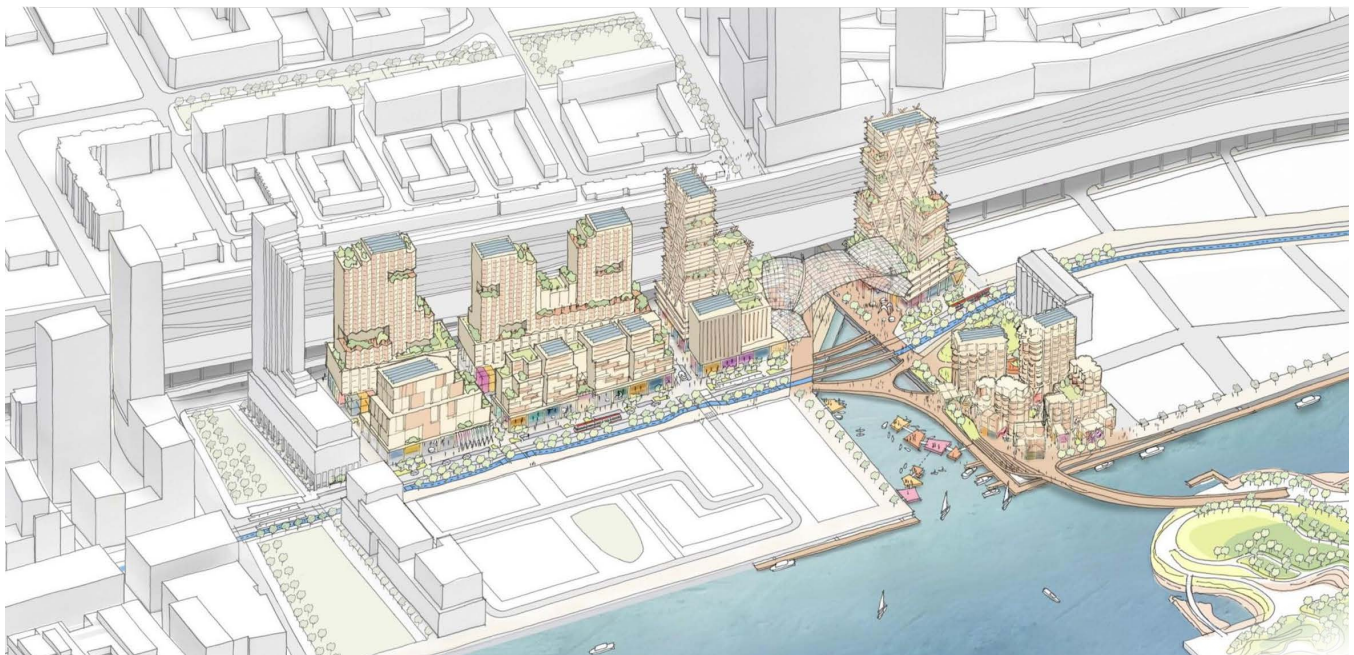
Energy Technologies Area
March, 2019



Disclaimer:

This document was prepared as an account of work sponsored by the United States Government. While this document is believed to contain correct information, neither the United States Government nor any agency thereof, nor the Regents of the University of California, nor any of their employees, makes any warranty, express or implied, or assumes any legal responsibility for the accuracy, completeness, or usefulness of any information, apparatus, product, or process disclosed, or represents that its use would not infringe privately owned rights. Reference herein to any specific commercial product, process, or service by its trade name, trademark, manufacturer, or otherwise, does not necessarily constitute or imply its endorsement, recommendation, or favoring by the United States Government or any agency thereof, or the Regents of the University of California. The views and opinions of authors expressed herein do not necessarily state or reflect those of the United States Government or any agency thereof or the Regents of the University of California.

Quayside Energy System Analysis



Michael Wetter and Jianjun Hu

March 21, 2019

Contents

1 Acknowledgments and Preamble	3
2 Executive Summary	4
3 Introduction	6
4 System	8
4.1 Bi-directional district heating and cooling	8
4.1.1 Discussion of basic configuration of bi-directional system	9
4.1.2 Attempt to control for zero differential pressure	11
4.2 Pressure-less bi-directional district heating and cooling	12
4.2.1 Control of the substation bypass	12
4.2.2 Control of the main plant bypass	13
4.3 Uni-directional district heating and cooling system with substations in series connection	13
4.3.1 Main functionality	14
4.3.2 Modular extension of the DHC	14
4.3.3 Connecting high and ambient temperature mesh	14
5 Model Description	16
5.1 District heating and cooling distribution	16
5.2 Energy Center	16
5.2.1 Sewage water heat recovery	18
5.2.2 Cooling towers	18
5.3 Substations	18
5.4 Geothermal field	20
5.5 Weather data, electricity price and greenhouse gas emission factor	21
5.6 Simulation model	21
6 Results	22
6.1 Simulated cases	22
6.2 Simulation Results	23
6.3 Analysis of the latest design change	28
6.3.1 Efficiency penalty	29
6.3.2 Comments on controllability and extensibility	31
6.3.3 Summary on design changes	31
7 Bibliography	32

Chapter 1

Acknowledgments and Preamble

We like to thank Sidewalk Labs which funded this work.

We like to thank Kerr Wood Leidal Associates Ltd. for providing the specification of the district energy system and borefields, and Integral Group for providing the load profiles and schematics of the substations. We like to thank Matthias Sulzer from EMPA Switzerland for the discussions about district energy system architectures.

This work was supported by the Assistant Secretary for Energy Efficiency and Renewable Energy, Building Technologies Office, of the U.S. Department of Energy under Contract No. DE-AC02-05CH11231.

This document was prepared as an account of work sponsored by the United States Government and Sidewalk Labs. While this document is believed to contain correct information, neither the United States Government nor any agency thereof, nor The Regents of the University of California, nor any of their employees, makes any warranty, express or implied, or assumes any legal responsibility for the accuracy, completeness, or usefulness of any information, apparatus, product, or process disclosed, or represents that its use would not infringe privately owned rights. Reference herein to any specific commercial product, process, or service by its trade name, trademark, manufacturer, or otherwise, does not necessarily constitute or imply its endorsement, recommendation, or favoring by the United States Government or any agency thereof, or The Regents of the University of California. The views and opinions of authors expressed herein do not necessarily state or reflect those of the United States Government or any agency thereof or The Regents of the University of California.

Chapter 2

Executive Summary

This report presents energy analysis for different district heating and cooling architectures for the Toronto Quayside development based on annual energy simulations. It also examines controllability and extensibility of different system architectures. The design goal for the Quayside development is to be climate positive.

First, we analyzed bi-directional energy systems that promise higher efficiency than unidirectional systems (see [Section 4.1](#)). However, it was reported by early installations, and confirmed by our simulations, that such systems experience pressure fluctuations that makes control difficult and thereby risks that heat pumps will have low or high pressure errors. To address this problem, LBNL developed in [Section 4.2](#) an improvement to bi-directional energy systems that avoids these pressure fluctuations. However, the modification compromises the flexibility to expand the bi-directional system. The bi-directional system is therefore not practical for the Toronto Waterfront. Finally, in [Section 4.3](#) we present a novel piping arrangement which we call uni-directional system with series connection. In its basic arrangement, discussed in [Section 4.3.1](#), substations are connected to a distribution ring in series. This series connection has various benefits over conventional uni-directional system in which substations are connected in parallel. In the series connection, substations have zero differential pressure. A pump draws water from the distribution ring to the substation. This hydraulically decouples the substations, which simplifies control as there are no pressure fluctuations in the district line if substations regulate their flow. Moreover, this arrangement can be modularly expanded ([Section 4.3.2](#)) and connected to higher temperature loads ([Section 4.3.3](#)). Both of these properties are valuable for the Toronto Waterfront as it facilitates the extension of the energy system and the addition of waste heat such as from the Redpath Sugar Refinery.

In [Section 6](#), we present results of annual energy simulations of the uni-directional system with series connection from [Section 4.3.1](#), and from the same system but with conventional parallel connection. It turns out that the series configuration lead to 1.4% less energy use and 1.3% less GHG emissions than the parallel configuration. We therefore recommend to use the series configuration, which is also easier to extend and control. For the geothermal fields, outlet temperatures are similar at the start and end of the year, indicating that they are properly controlled. The biggest energy savings are achieved if the design water temperature for space heating is reduced from 41°C to 30°C, and the design water temperature for space cooling is raised from 4°C to 10°C. The energy savings are 12.0% for a decrease in heating temperature, 8.6% for a raise in cooling temperature, and 20.7% for the combined change in heating and cooling temperatures. Increasing the heat exchanger effectiveness from 71% to 90% has no noticeable effect. Reducing the number of boreholes, either by reducing the overall area by 20% or by increasing the spacing between the drillings by a factor of $1/\sqrt{0.8} = 1.12$, which leads to the same number of boreholes, increases energy consumption by 3.4%. Either reducing the overall bore-field area by half or increasing the spacing by a factor of $1/\sqrt{0.5} = 1.41$, which leads to the same number of boreholes, increases energy consumption by 12.7%. Hence, a moderate reduction of the number of boreholes could be an effective

measure to reduce costs.

While the simulations were conducted, the design team significantly changed the energy system by moving the borefields from the substation to the district loop, operating them with subfreezing temperatures, and changing the substation hydraulic.

The design team proposed a further modification to the unidirectional system in which the borefields were moved from the substations to the district loop, the substation hydraulic was changed, and the borefield operated with subfreezing temperatures. In [Section 6.3](#) we estimate the impact on energy use, based on a 2nd Law of Thermodynamics analysis, and we comment on controllability and extensibility of the new design. We estimate that the new design requires about 40% more energy due to the higher temperature lift between borefield and load, and due to the additional heat exchangers that cause second law inefficiencies which need to be compensated for with compressor energy. The resulting increase in energy costs is estimated to be around \$180 k/a, and the increase in GHG emissions is estimated to be around 0.07 kt/a. In addition, the new design leads to a more complex hydraulic and to cascading control loops, which makes it harder to operate the system at its peak performance and ensure its efficiency during its lifetime.

Chapter 3

Introduction

Waterfront Toronto and Alphabet's Sidewalk Labs are creating a new kind of mixed-use, complete community on Toronto's Eastern Waterfront, beginning with the creation of the Quayside area. The team's goal is to create a flexible and expandable system that can grow to support new development and neighborhoods beyond the project.

The design goal for the Quayside development is to be climate positive. Heating and cooling will be provided through a district heating and cooling (DHC) system that integrates waste heat utilization, geothermal storage and heat pumps for heating, cooling and waste heat utilization.

To support the design of the thermal system, energy simulations of the buildings and of the DHC system have been conducted, using input from the design team which is comprised of KWL Engineering and Integral Group. This report is concerned with the performance of the DHC system, taking as input hourly load profiles from the building load simulations that were conducted by Integral Group, and specifications for the DHC distribution provided by KWL Engineering. The objective of the analysis is to understand the suitability of different design alternatives for the DHC distribution system through analysis of their energy and greenhouse gas performance, hydraulic behavior and controllability. To conduct the analysis, dynamic, annual simulations of the DHC system, of the geothermal fields and of the substations have been conducted.

A starting point for the system architecture was bi-directional DHC systems. These systems are in their early stage of research and development. They have been shown to have higher exergy performance than standard uni-directional systems [SKrauchiS15]. Few of these installation are in construction or operation [Gau15], or have been monitored [VS15]. Because of the small temperature lifts and their dynamic operation, these systems are sensitive to how they are controlled [BunningWFMuller18]. Recent research also shows that uni-directional DHC systems in which substations are connected in series have similar energy performance but lead to differential-pressure distributions that are easier to control [SSS18].

Therefore, to better understand the performance and dynamic behavior of such different DHC system architectures, this study built simulation models of different architectures to analyze their behavior, selected what the design team thinks are the best suited configurations for the Quayside development, and then conducted annual simulations.

To built the models, the equation-based, object-oriented Modelica modeling language has been used [ME97]. We used component models, such as for heat pumps, geothermal fields, circulation pumps, valves, pipes and storage tanks and basic control blocks from of the Modelica Buildings Library [WZNP14]. These were assembled to form system models, including supervisory control sequences. Based on hourly weather data and hourly load profiles for one year, these models simulate the thermal behavior, pressure and mass flow distribution of the equipment, the geothermal fields and

the piping network, as well as the supervisory control of all substations and the central plant, using idealized local loop control.

The remainder of this report is structured as follows: [Section 4](#) discusses different topologies for DHC distribution networks, [Section 5](#) describes the models that we implement to conduct annual simulations, [Section 6](#) presents the results.

Chapter 4

System

This section describes different system architectures for district heating and cooling distribution networks. It presents bi-directional district heating and cooling systems, a modification to these systems that avoids fluctuations in differential pressure at the substations, and finally it presents uni-directional systems in which substations are coupled in series to the distribution loop.

4.1 Bi-directional district heating and cooling

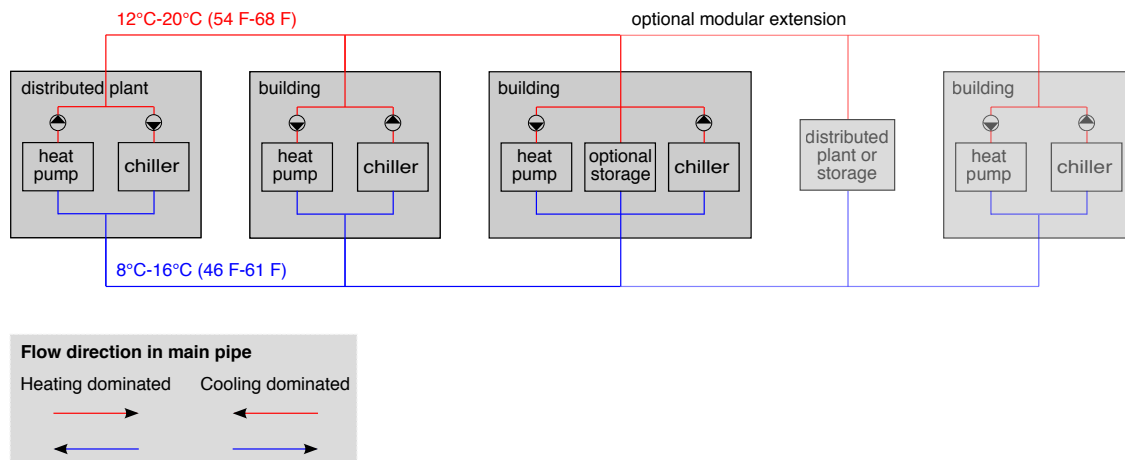


Fig. 4.1: Bi-directional thermal network.

In bi-directional district heating and cooling systems, shown schematically in Fig. 4.1, substations have pumps that draw water from a warm line when in heating mode, or a cool line when in cooling mode. The distribution line, shown horizontally in the figure, is a large, typically non-insulated, pipe. If all buildings in the figure were in heating mode, the flow would be in clockwise direction, and if all buildings were in cooling mode, the flow would be counter-clockwise. Hence, in the distribution line, the direction of flow changes. If all substations were balanced, then no flow would go through the plant, shown in the left of the figure. Otherwise, there is flow through the plant, and the plant is controlled to stabilize the temperature within certain ranges.

The Swiss Competence Center for Energy Research, Future Energy Efficient Buildings & Districts (SCCER-FEEBD), built and monitored several bi-directional DHC systems. In installed systems, control problems and cavitation in pumps caused by large pressure drops across consumers have been observed [Sul18].

4.1.1 Discussion of basic configuration of bi-directional system

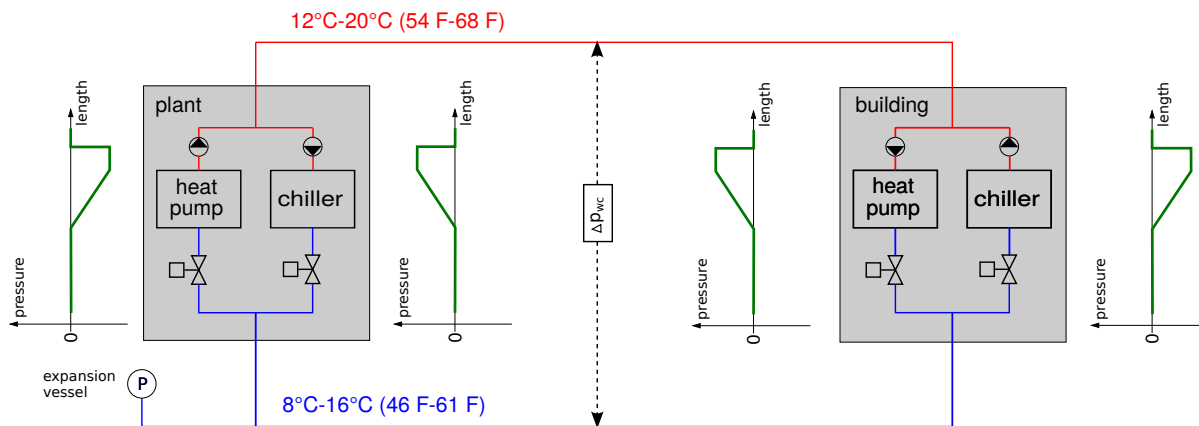


Fig. 4.2: Bi-directional thermal network with pressure balance for the situation where $\Delta p_{wc} = 0$.

We will now explain why we believe the observed control problems are a fundamental property of bi-directional DHC systems. Consider the simple system shown in Fig. 4.2 with one plant on the left, and one substation of a building with heating and cooling on the right. The plant and each building substation has circulation pumps whose pump head is equal to the flow friction of the heat pump or chiller and the control valve. For simplicity, suppose the pressure drop of the distribution pipes is negligible compared to the pressure drop of the substation. Then, the pressure distribution shown in green result across the heat pump and chiller flow segments. Now, suppose each substation is controlled to provide a temperature difference between warm and cold intake/supply of 4 Kelvin. Furthermore, suppose that the pumps and compressors have variable frequency drives that allow the pump to be reduced to 20% of the design flow rate, and similarly, suppose that the heat extracted or added by the substation can be reduced to 20% of the design heat flow rate. Suppose the pumps in the substation are oversized, which is a common situation. Consider the operation point where in the substation, the chiller is off and the heat pump reduces its compressor speed to the minimum, i.e., the substation extracts only 20% of the evaporator's design heat flow rate. Then, to maintain the 4 Kelvin temperature drop, the water pump needs to be controlled to its minimum speed, which requires the control valve to be adjusted because of the oversized pump. As the valve modulates, the pressure in the warm pipe changes (because the cold pipe is connected to the expansion vessel and hence has constant pressure). Because pressure is propagated nearly instantaneous (at the speed of sound), the pressure across the whole warm pipe is changing. If there are more than one substation connected, then all substations would have to compensate for this pressure change by adjusting their pump speed and/or valve position. However, because compressor speed, pump speed and valve motors have all a similar time constant, there is no time scale separation. Furthermore, because pressure is propagated nearly instantaneous through incompressible flow, all control loops that regulate mass flow rate or pressure are tightly coupled. Therefore, it is likely that the substations start to hunt, and if the control becomes unstable, large water flow variations can cause high or low pressure errors in the heat pumps. Based of this discussion, we do not believe that it is practical to tune the control in a way that ensures stable operation.

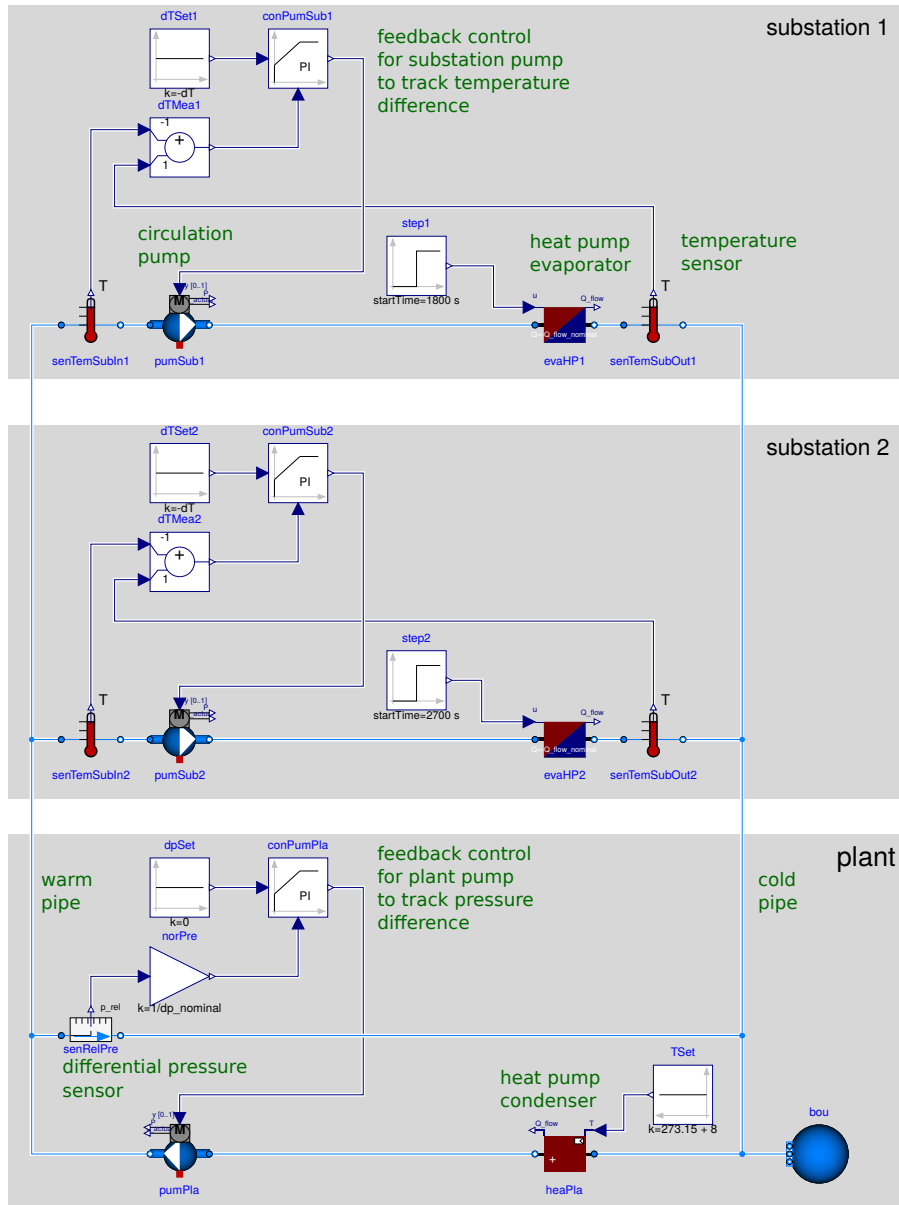


Fig. 4.3: Modelica model that reproduces the pressure propagation through the bi-directional system.

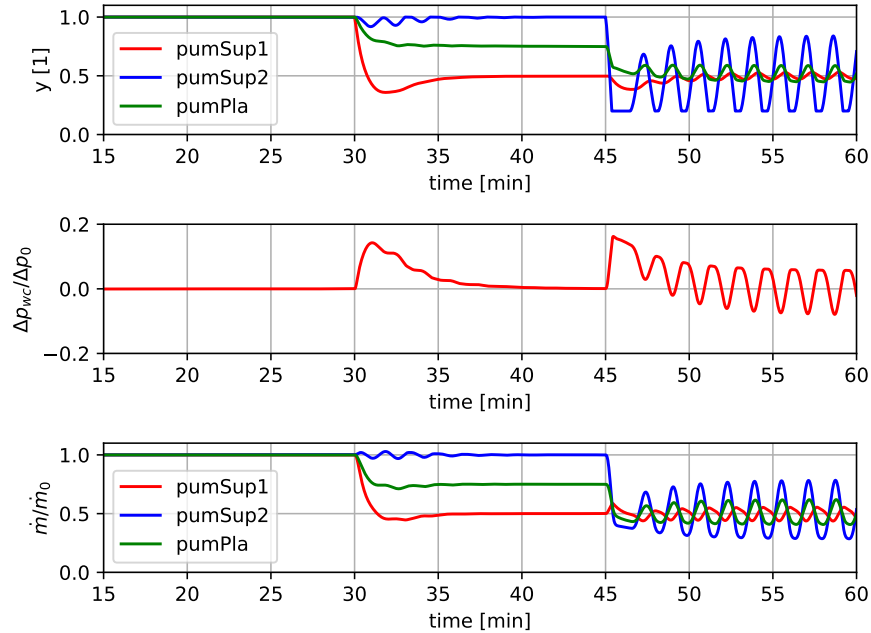


Fig. 4.4: Time trajectories that illustrate the pressure fluctuation for the case where one substation controller is unstable. Plot produced using the model shown in Fig. 4.3.

4.1.2 Attempt to control for zero differential pressure

As a work-around, one may attempt to control for zero differential pressure across the warm and cold pipe. The controlled variable would be the pressure difference labeled Δp_{wc} in Fig. 4.2, measured somewhere in the distribution pipes, and the actuated variables would be the pumps in the plant on the left hand side in the figure. However, such a system also suffers from the same lack of time scale separation. To confirm this statement, we built the simplified model shown in Fig. 4.3. Here, we only implemented the components used if there is only heating demand. The system has two building substations, with the heat pump evaporators labeled $evaHP1$ and $evaHP2$, and one heating plant, which we idealized by the energy source labeled $heaPla$ which heats water to a constant temperature of 8°C . The system is configured for a design pressure drop of 30 kPa in the building substation and the plant. Fig. 4.4 shows the time trajectories for the pump control signals, for Δp_{wc} , and for the water flow rate through the substations and the plant for the scenario where the load is reduced from the design load to 50% of the design load at $t = 30$ minutes and at $t = 45$ minutes for $evaHP1$ and $evaHP2$, respectively. For this scenario, we tuned the controller for the substation 2 to be unstable. The plot with the mass flow rate distribution shows how this instability is propagated through the system. Between $t = 30$ minutes and $t = 45$ minutes, the control is asymptotically stable, e.g., it reaches steady-state. However, for $t > 45$ minutes, the control is unstable. The instability from one substation propagates throughout the system because the tightly coupled dynamics that have similar time rate of changes. Therefore, we doubt that it will be practical to achieve stable control.

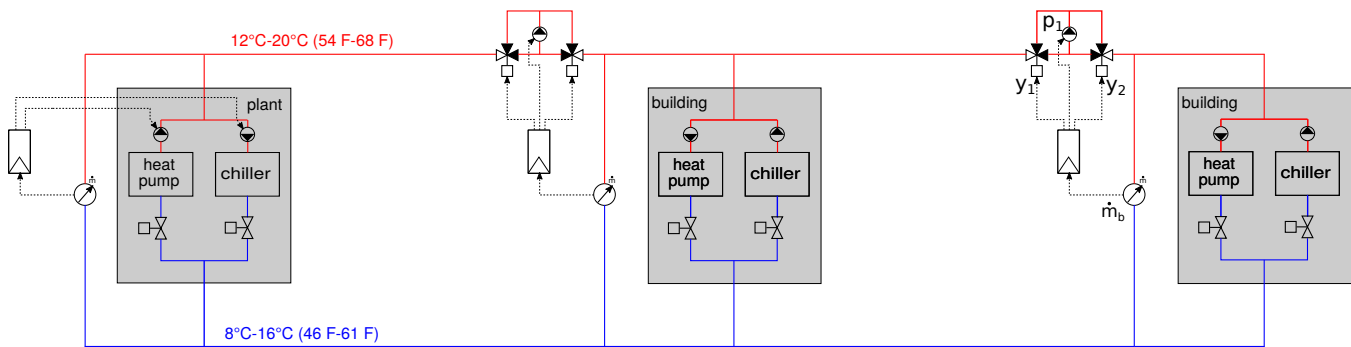


Fig. 4.5: Pressure-less bi-directional thermal network.

4.2 Pressure-less bi-directional district heating and cooling

As controlling for zero differential pressure is difficult to achieve, we will now present a modification to the bi-directional system that has the following properties:

1. Each substation has zero differential pressure, and
2. if there is no control error, then there is no mixing between the warm and cold pipe.

Property 1 ensures controllability of the mass flow rate through the heat pumps in the substations, in particular satisfying the minimum flow rate required for proper operation of heat pumps. Property 2 ensures that exergy is preserved, thereby reducing system-level electricity consumption. Fig. 4.5 shows the new configuration. At each substation, we added a bypass between the warm and cold pipe to ensure property 1, and we added a pump and control valves in the warm pipe to ensure property 2. The design is modular, with each of these configurations added to a substation connection. (If substations are close to each other, then they may share such a configuration consisting of bypass, pump, valve and control loop.) The bypass has a flow measurement that measures the mass flow rate \dot{m}_b through the bypass, where \dot{m}_b is defined as positive if the flow is from the warm to the cold line.

4.2.1 Control of the substation bypass

The pump and valves at the by-pass of the substations are controlled to track $\dot{m}_b = 0$. Let \dot{m}_0 be the design mass flow rate for the flow rate of the pump P1. The control sequence is as follows: Let $e = \dot{m}_b / \dot{m}_0$ be the control error.¹ The pump speed y_p and the valve lifts y_1 and $y_2 = 1 - y_1$ are controlled based on the output $y_c \in [-1, 1]$ of a proportional-integral (PI) controller as shown in Fig. 4.6, where a valve lift of 1 means that the bypass port is closed, indicated by a black filled triangle.

With this control sequence, if there is mass flow from the warm to the cold line, then $\dot{m}_b > 0$ and hence y_c increases due to the integral action of the PI control law $y_c = K_p e + K_i \int_0^t e(s) ds$, where $K_p > 0$ and $K_i > 0$ are control gains. While y_c increases, if $-1 \leq y_c \leq -0.1$, the pump speed is reduced to its minimum. Next, the valves open and close as y_c traverses -0.1 to $+0.1$ (adjustable). Next, as $y_c > 0.1$, the pump speed increases. At steady-state, there is no control error because of the integral action of the PI controller, and hence the bypass mass flow rate is $\dot{m}_b = 0$. In the limiting case of $y_c = 0$, the pump is at minimum speed, there is no flow in the distribution pipe, and all flow of the pump is recirculated. Pump energy will be low at this operating point as the pump energy is cubic to the volume flow rate. However, to prevent overheating of

¹ We divided by the design flow rate to normalize the control input and hence simplify the tuning of the controller.

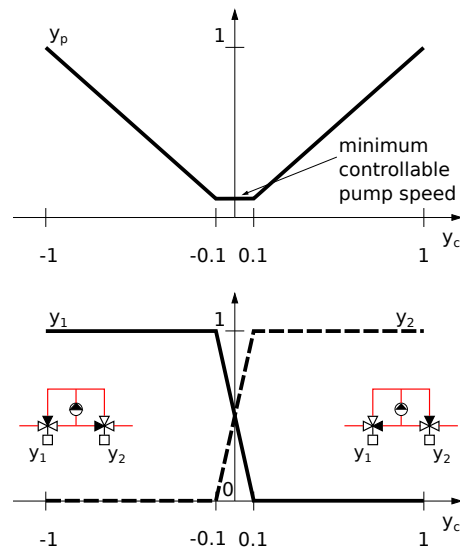


Fig. 4.6: Control chart for the pump speed and control valves for the pressure-less bi-directional system.

the pump, the motor must be air-cooled and the pipes be non-insulated. The pump must be sized for the design flow rate and flow friction of the distribution leg in which it is installed.

Note that as in Section 4.1.2, instabilities of the pump control loop will be propagated to other pump control loops due to conservation of mass. However, in contrast to the system of Section 4.1.2, the differential pressure across each substation will always be zero (due to the bypass). Hence, ensuring minimum and stable flow rate through the heat pumps is not a problem, as the heat pump controller will only have to compensate for variations in temperature. However, note that if the district energy system is expanded to serve additional development and neighborhoods along the Toronto Waterfront, then the pumps and control valves may have to be replaced with larger ones.

4.2.2 Control of the main plant bypass

The main plant, shown on the left in Fig. 4.5 requires no additional control valves. Rather, the pumps of the heat pumps or the heat recovery units are controlled, in priority, such that (i) the minimum flow rate is satisfied, and (ii) the bypass has zero mass flow rate. To control the bypass mass flow rate, a PI controller needs to be used to ensure zero flow rate in the by-pass (provided that the minimum flow rate can be satisfied).

4.3 Uni-directional district heating and cooling system with substations in series connection

Due to the hydraulic problems of bi-directional DHC systems, Sulzer et al. [SSS18] studied so-called uni-directional DHC networks which we described in this section. The authors state that a uni-directional system in which substations are connected in a series configuration has, compared to the bi-directional system, a 4% higher electricity consumption in heating-only mode, and a similar electricity consumption if heating and cooling loads are balanced. Thus, on an annual basis, both systems are expected to have comparable energy performance. The primary advantage of the uni-directional

system with series connections is that it does not suffer from the hydraulic control problems. The uni-directional system also allows a modular extension through the addition of meshes, and thus is suited for developments that are built out in stages.

4.3.1 Main functionality

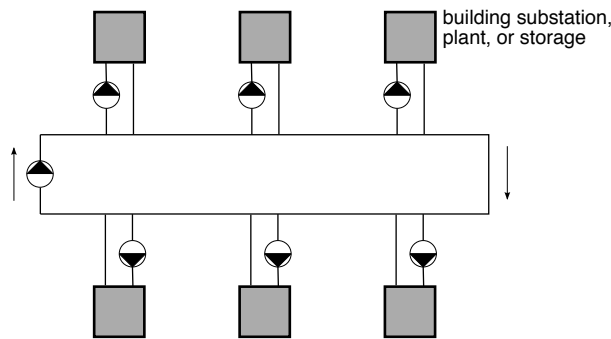


Fig. 4.7: Uni-directional system. (Figure reproduced from [SSS18].)

We will now describe the uni-directional DHC system shown in Fig. 4.7. In this system, the water circulates in the main loop, which we will call *mesh*. Each consumer, plant or storage, which we will below call *load* is connected to the mesh as shown in the figure. The distance between the inlet and outlet of each load is kept small and therefore there is no pressure drop across inlet and outlet of the load. This decouples each load hydraulically from flow variations in the mesh. This hydraulic decoupling is one of the key differences compared to the bi-directional system. However, thermally, the loads are coupled, but this is from a control point of view simple to handle because of the thermal inertia of the mesh, and because by design, the temperature variations across the mesh are kept small. The pipe of the mesh is buried in the ground and typically uninsulated, which further increases the energy storage potential of the mesh (which may be exploited to shift peak demand), increases its thermal inertia and reduces material costs. To keep the pressure drop low, the mesh may be sized for a pressure drop of 100 Pa/m (depending on the size and elevation of the system). Other design variables include a temperature difference of 4K along the mesh and across each load. The mesh may be controlled to a minimum of 8° C (to avoid freezing in a heat pump evaporator) and a maximum of 16° C (to allow for free-cooling in a building).

4.3.2 Modular extension of the DHC

Within the existing footprint of the DHC system, the DHC system can be extended by adding more buildings, plants or storage to the mesh. To serve a larger area, multiple meshes can be hydraulically coupled as shown in Fig. 4.8. By controlling the main pump of the meshes, excess waste heat can be transported from one mesh to another.

This modular extensibility allows the main mesh to be sized for Quayside. Should the DHC system later be extended to serve other areas of the Toronto Waterfront, then additional meshes can be connected as shown in the figure.

4.3.3 Connecting high and ambient temperature mesh

If waste heat is available at temperatures above the maximum mesh temperature (of say 16°C), then it can be provided through a separate high temperature mesh. Heat from this high temperature mesh could be used to directly serve space

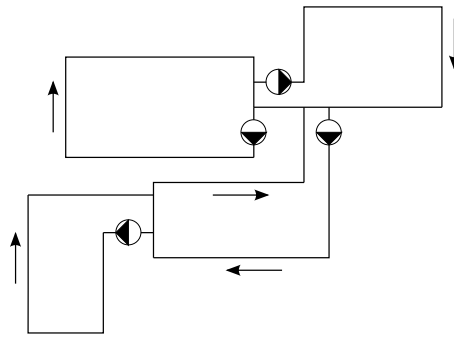


Fig. 4.8: Extension of uni-directional system to couple hydraulically multiple meshes. (Figure adapted from [SSS18].)

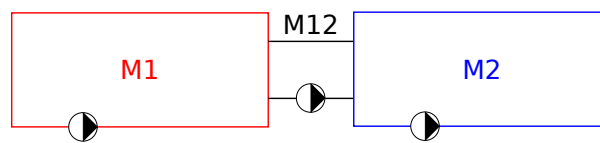


Fig. 4.9: Extension of uni-directional system to couple meshes of different temperatures. (Figure reproduced from [SSS18].)

heating or to (pre-)heat domestic hot water. The high and ambient temperature meshes will have loads connected as shown in Fig. 4.7. To transport excess heat from the high temperature mesh $M1$ to the ambient temperature mesh $M2$, they can be connected as shown in Fig. 4.9. The pump in the connection $M12$ can be controlled to exchange heat between the two meshes.

Connecting high and ambient temperature meshes as shown in Fig. 4.9 allows for example to operate a high temperature mesh that transports waste heat from local industrial plants, if such an opportunity became available.

Chapter 5

Model Description

This section describes the model that was used for the simulation-based analysis.

5.1 District heating and cooling distribution

We investigated two types of uni-directional systems, shown in Fig. 5.1 and Fig. 5.2. The difference is that the substations connect with the district system either in parallel or series. We therefore call these variants parallel uni-directional system and series uni-directional system.

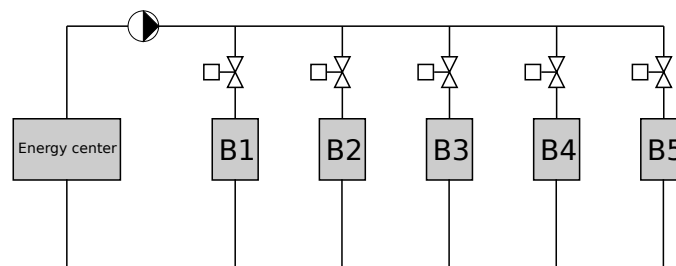


Fig. 5.1: Parallel uni-directional system.

5.2 Energy Center

The energy center shown in Fig. 5.3 includes a sewage heat recovery heat exchanger to harvest waste heat from sewage water for heating, cooling towers for cooling, and an auxiliary heating and cooling source to ensure sufficient heating and cooling supply.

The sewage heat exchanger and the cooling towers are operated to maintain the district water supply temperature to be higher than 12°C in winter and lower than 40°C in summer, subject to sufficient capacity. The setpoint is shown in Fig. 5.4. Auxiliary heating and cooling sources are activated if the temperature becomes higher than 42°C or lower than 10°C.

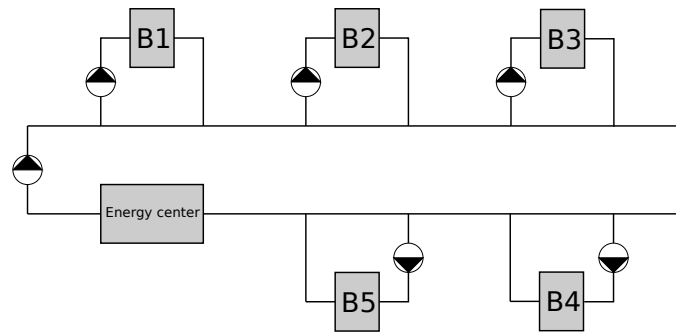


Fig. 5.2: Series uni-directional system.

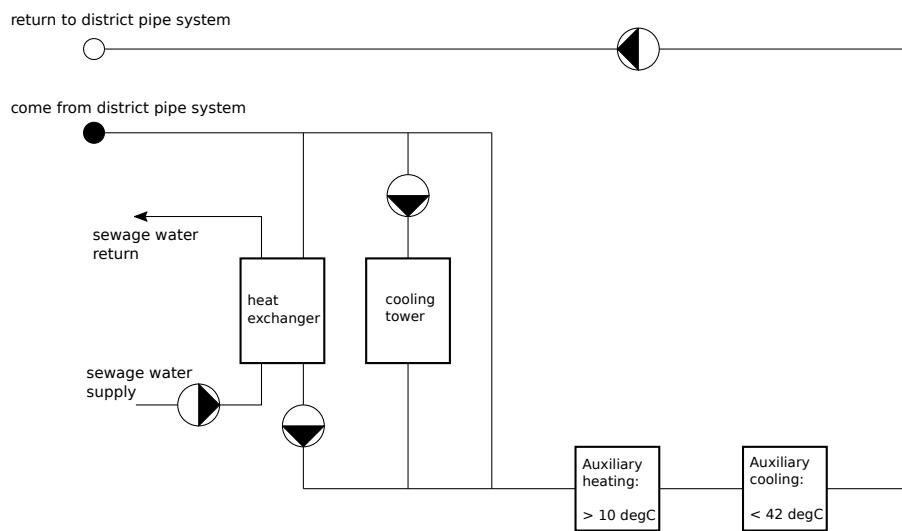


Fig. 5.3: Energy center including sewage heat exchanger, cooling tower, and auxiliary heating and cooling source.

In the model, these auxiliary heating and cooling sources are idealized and are agnostic to the type of heating or cooling technology.

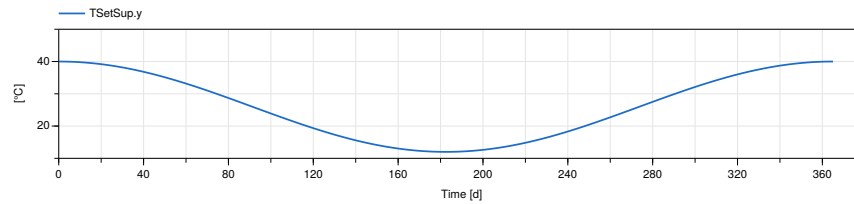


Fig. 5.4: Temperature setpoint for leaving district water.

5.2.1 Sewage water heat recovery

The simulations assumed a sewage water temperature of 15°C in winter and 25°C in summer, varied as shown Fig. 5.5. The speed of the sewage heat exchanger pumps are controlled to meet the district water temperature setpoint shown in Fig. 5.4.

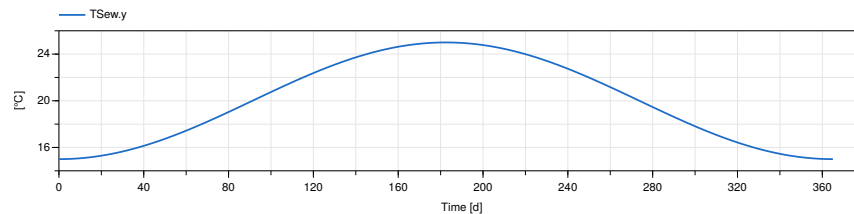


Fig. 5.5: Sewage water temperature.

5.2.2 Cooling towers

We assumed the cooling towers have an approach temperature of 2 Kelvin. Pumps and fans in the cooling tower loop are controlled to cool the district water to the setpoint shown in Fig. 5.4.

5.3 Substations

Fig. 5.6 shows the substation with its main four main parts: a heating load and a cooling load, a centralized WSHP, and a source that uses the geothermal field or the district loop. Buffer tanks prevent that a change in pump speed in one of these parts causes changes in differential pressures in other parts of the system. A water source heat pump (WSHP) boosts the temperature up or down, and allows for direct heat recovery during simultaneous heating and cooling operation within a substation.

Fig. 5.7 shows the setpoints of hot water supply and return temperatures. The setpoints are reset based on outdoor air temperature. The maximum supply water temperature is 41°C when the outdoor temperature is -10°C , and decreases to 25°C at 15°C outside temperature. The difference between supply and return is 5°C.

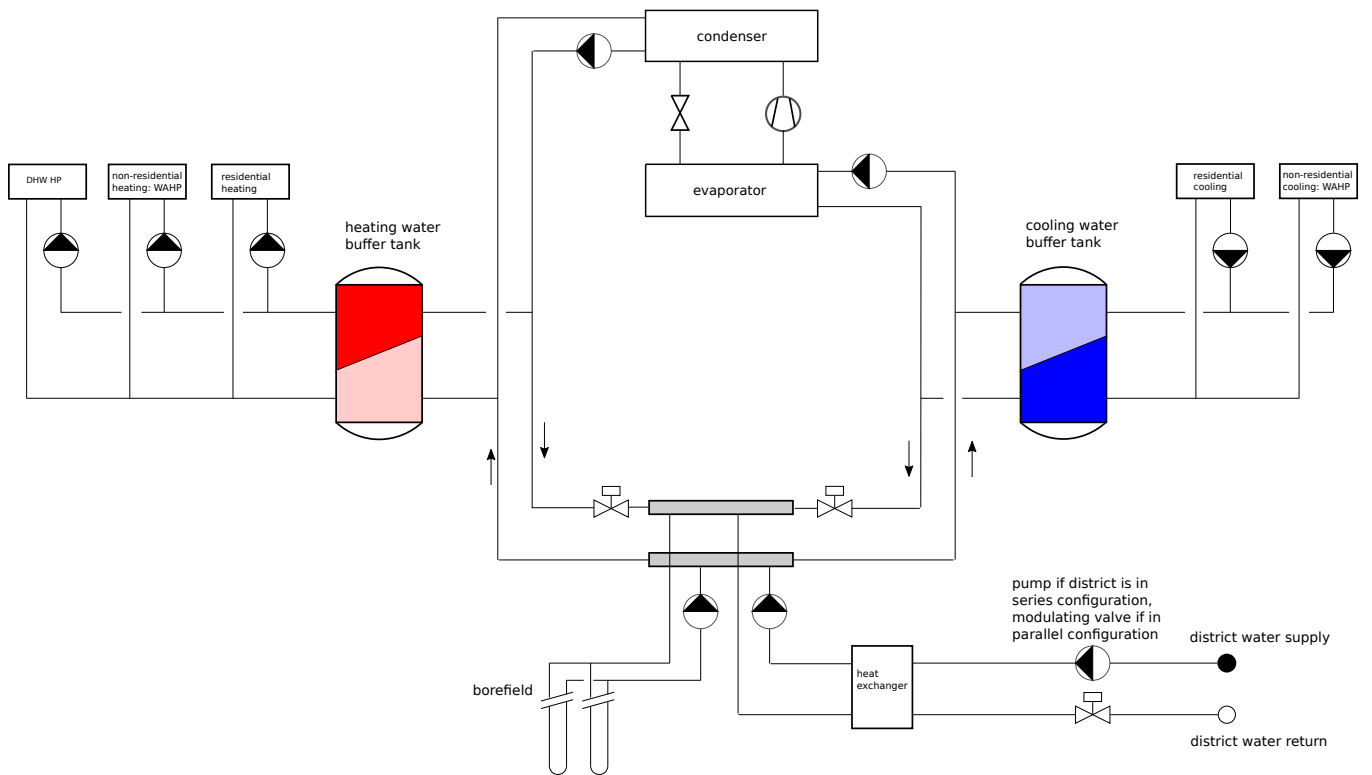


Fig. 5.6: Schematic diagram of the substations.

Using hourly load profile for heating and cooling, the water mass flow provided to the loads was controlled to be

$$\dot{m} = \frac{\dot{Q}}{c_p \Delta T}, \tag{5.1}$$

where \dot{Q} is the load, c_p is the specific heat capacity of water, and ΔT is the difference between supply and return water setpoint temperature.

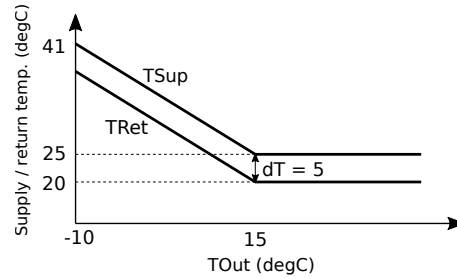


Fig. 5.7: Space heating supply and return water temperatures.

Fig. 5.8 shows the temperature setpoint for the cooling supply water to the load. The setpoint is reset based on the outdoor absolute humidity. If the humidity is high, dehumidification is likely not required in which case the chilled water temperature can be raised to increase the coefficient of performance of the heat pump. The water mass flow rate to the load was controlled in the same way as for the heating load, with a fixed temperature difference $\Delta T = 5$ Kelvin.

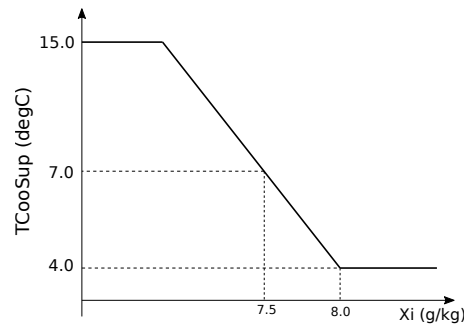


Fig. 5.8: Cold water supply setpoint.

5.4 Geothermal field

Table 5.1: Borefield data.

Building	Borefield length m	Borefield width m	Number of holes
1	35	44	72
2	45	50	110
3	20	40	45
4	35	40	72
5	60	40	117
Total			416

Each of the five substations has a geothermal field with dimensions and number of boreholes as shown in [Table 5.1](#). The boreholes are spaced 5 meters apart from each other and have a depth of 245 meters.

The heat exchange with the geothermal field is simulated using a dynamic model that computes the change in soil temperature based on the extracted or injected heat, and based on the geometry and soil properties of the borefield.

5.5 Weather data, electricity price and greenhouse gas emission factor

We used hourly weather data from Typical Meteorological Year TMY3 for Toronto [\[WM08\]](#). We used an electricity price of 0.089 \$/kWh. We used a greenhouse gas emission factor of 0.036 kg/kWh for electricity, which was obtained from [\[Tor18\]](#).

5.6 Simulation model

The models are implemented using the Modelica Buildings library [\[WZNP14\]](#), master branch, commit [45d5551](#). The system model consists of 9,000 component models, 40,000 equations, 11,000 time varying variables and 580 continuous time states.

For the simulations, we used Dymola 2019 FD01 with the Ccode solver and a tolerance of 10^{-6} . The sparse solver was activated. To reduce the size of the output file, we did not store variables at events. The number of output intervals was set to 500.

Chapter 6

Results

6.1 Simulated cases

Table 6.1 shows the cases that have been simulated. The impact of the following parameters changes was analyzed.

- Use of the series or parallel uni-directional district system.
- Change in design heating water temperatures at the loads from 41/30°C to 30/25°C.
- Change in design cooling water temperatures at the loads from 4 ... 15°C (reset based on outdoor humidity) to 10 ... 18°C (with same reset strategy).
- Change in design heat exchanger effectiveness from 71% to 90%.
- Change in the length of the geothermal fields to 80% or 50% of their original lengths, respectively. For this change, the distance between boreholes was kept constant, thereby reducing the number of boreholes.
- Change in the distance between the boreholes to $1/\sqrt{0.8} = 1.12$ or $1/\sqrt{0.5} = 1.41$ of its original distance, respectively. For this change, the areas of the geothermal fields are kept constant, thereby again reducing the number of boreholes to the same number as in the above case.

The performance of each setting was evaluated based on the annual energy use, energy cost and green house gas emissions.

Table 6.1: List of simulated cases.

Case	T_{heaSup} (°C)	T_{heaRet} (°C)	T_{cooSup_min} (°C)	T_{cooSup_max} (°C)	eps	$geoLenSca$	$geoHDisSca$
uniSer	41	30	4	15	0.71	1	1
uniPar	41	30	4	15	0.71	1	1
uniSer_THeaSup	30	25	4	15	0.71	1	1
uniSer_TCooSup	41	30	10	18	0.71	1	1
uniSer_THeaCooSup	30	25	10	18	0.71	1	1
uniSer_eps	41	30	4	15	0.9	1	1
uniSer_borAre20	41	30	4	15	0.71	0.8	1
uniSer_borAre50	41	30	4	15	0.71	0.5	1
uniSer_borDis20	41	30	4	15	0.71	1	$1/\sqrt{0.8}$
uniSer_borDis50	41	30	4	15	0.71	1	$1/\sqrt{0.5}$
uniSer_all20	30	25	10	18	0.9	0.8	1
uniPar_all20	30	25	10	18	0.9	0.8	1
uniSer_all50	30	25	10	18	0.9	0.5	1
uniPar_all50	30	25	10	18	0.9	0.5	1

6.2 Simulation Results

Table 6.2: Load in each building.

Building	Q_{coo} [kWh/(m ² a)]	Q_{hea} [kWh/(m ² a)]	Q_{dhw} [kWh/(m ² a)]
1	-30.52	46.47	29.99
2	-27.94	48.41	26.35
3	-18.99	35.42	17.44
4	-23.57	39.66	22.45
5	-37.09	61.05	35.58

Table 6.2 shows loads in each building, including space cooling, space heating and domestic hot water heating.

Fig. 6.1 shows for the base case with series configuration the main temperatures in the substation 1. The water temperatures into and out of the borefield, T_{inBor} and T_{outBor} , shows that their difference is quite significant in periods between the heating and cooling seasons. This indicates that the geothermal system stores heat during cooling season and releases it at winter. The borefield outlet water temperature T_{outBor} is similar at the beginning and end of the year, which indicates that the borefield is properly operated. The middle and bottom figure shows that the control ensures that during heating season and cooling season, the top of the heating tank $T_{heaTanTop}$ and the bottom of the cooling tank $T_{cooTanBot}$ follows their respective setpoints $T_{heaSupSet}$ and $T_{cooSupSet}$.

Fig. 6.2 shows that for January, February and December, auxiliary heating is required. The figure also shows that no cooling is required from the cooling towers or the auxiliary cooling.

Fig. 6.3 compares the energy consumption for the base case with the series and parallel configuration. There is no significant difference between them. The plot also shows that geothermal system can satisfy all the cooling load and no cooling supply needs to be provided from the district loop.

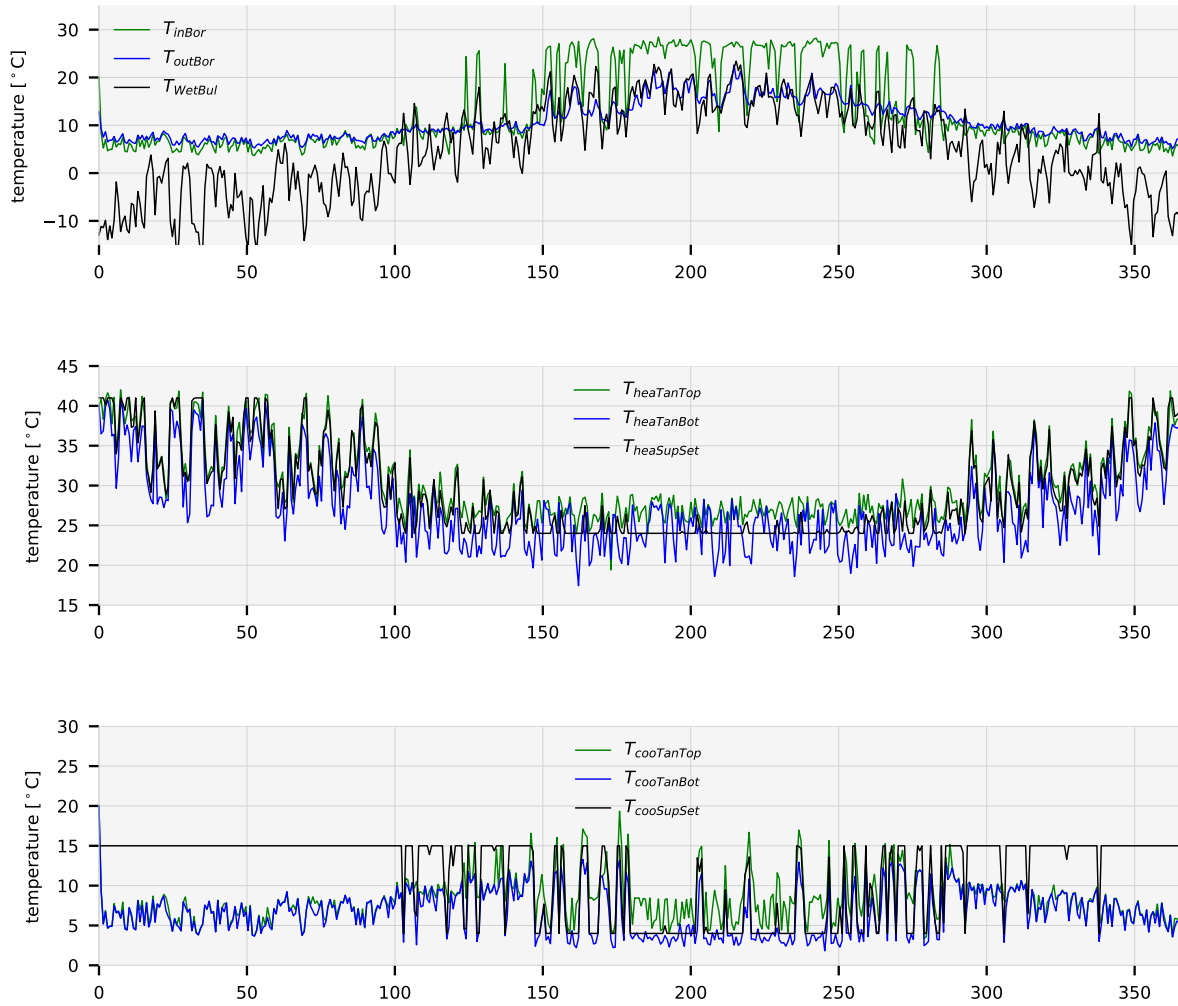


Fig. 6.1: Temperature profiles in substation 1 for the base case with the series configuration.

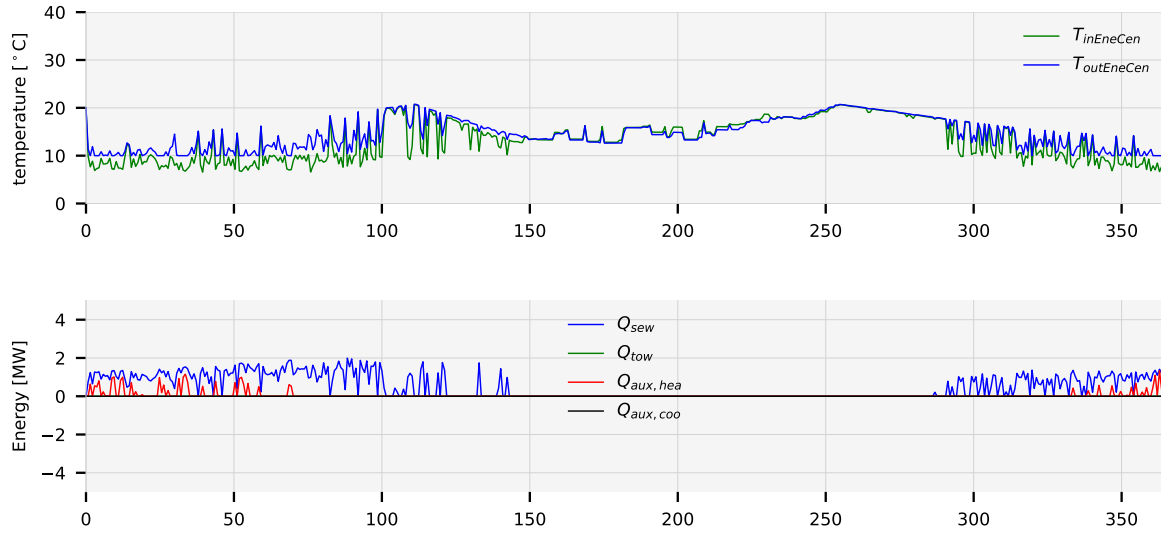


Fig. 6.2: Water temperatures in and out, energy in and out at central energy center, for the base case with series connection. Around 240 days, there is a temperature difference between inlet and outlet, but zero energy consumption. This is because the energy is provided by the cooling towers.

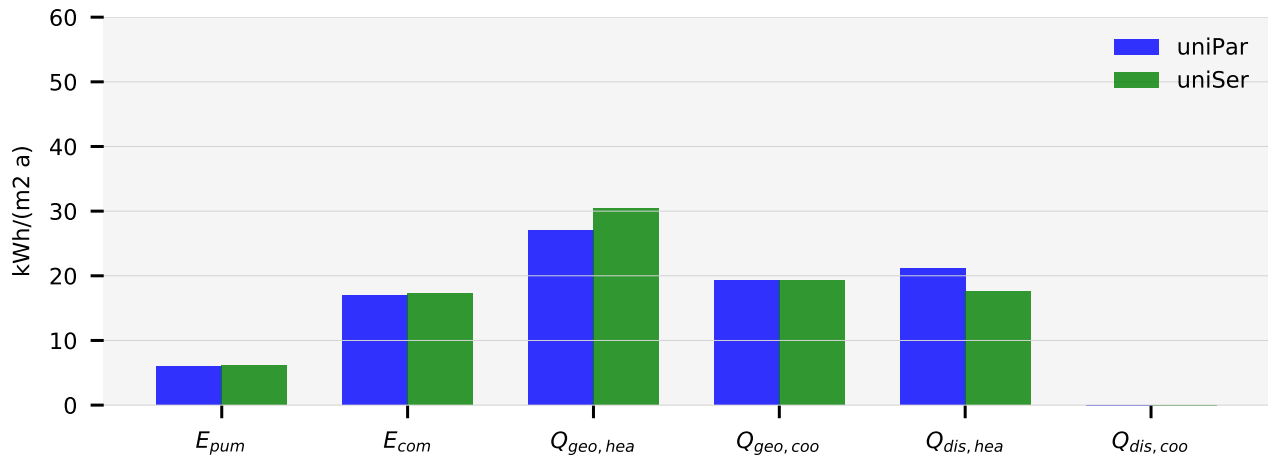


Fig. 6.3: Energy break-down in substation 1 for the base cases with the series and parallel configuration.

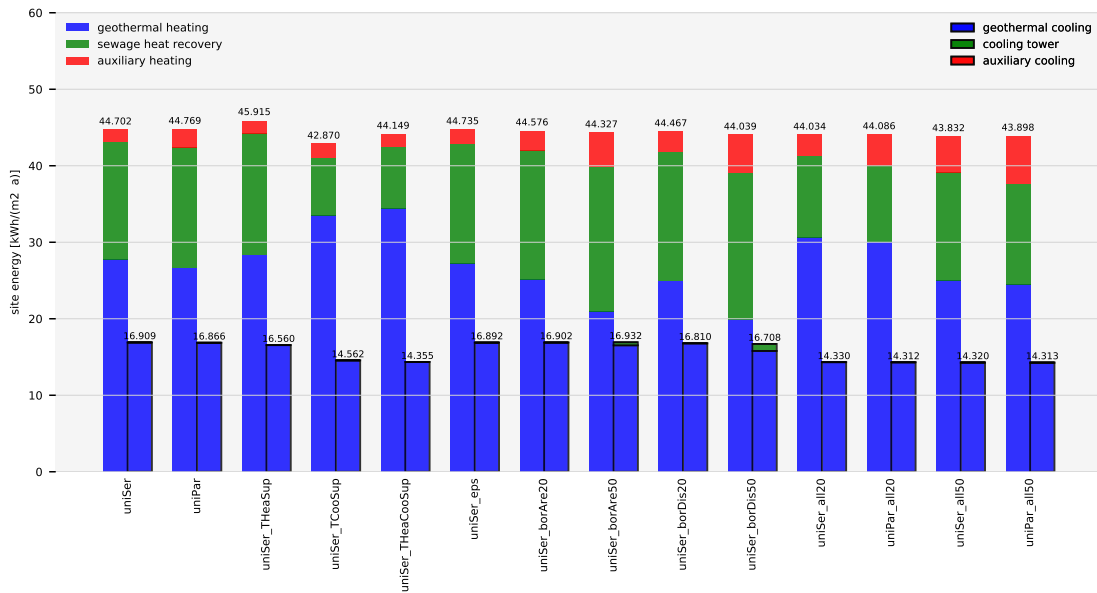


Fig. 6.4: Energy break-down for all simulated cases.

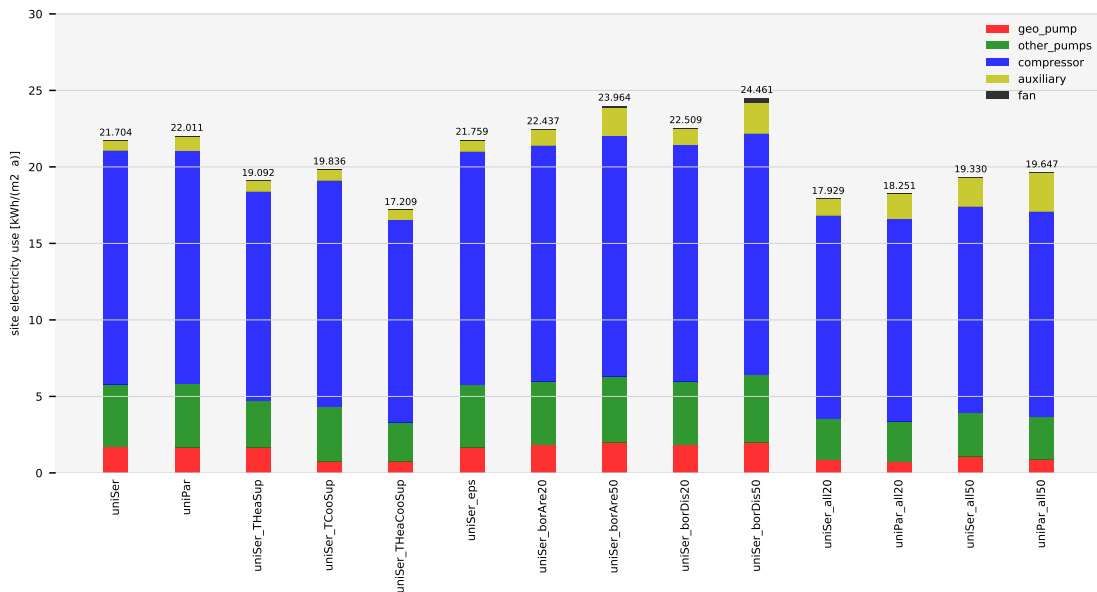


Fig. 6.5: Annual site electricity use for all simulated cases. Auxiliary heat added at the central plant was assumed to be supplied by an air to water heat pump with $COP_h = 2.5$.

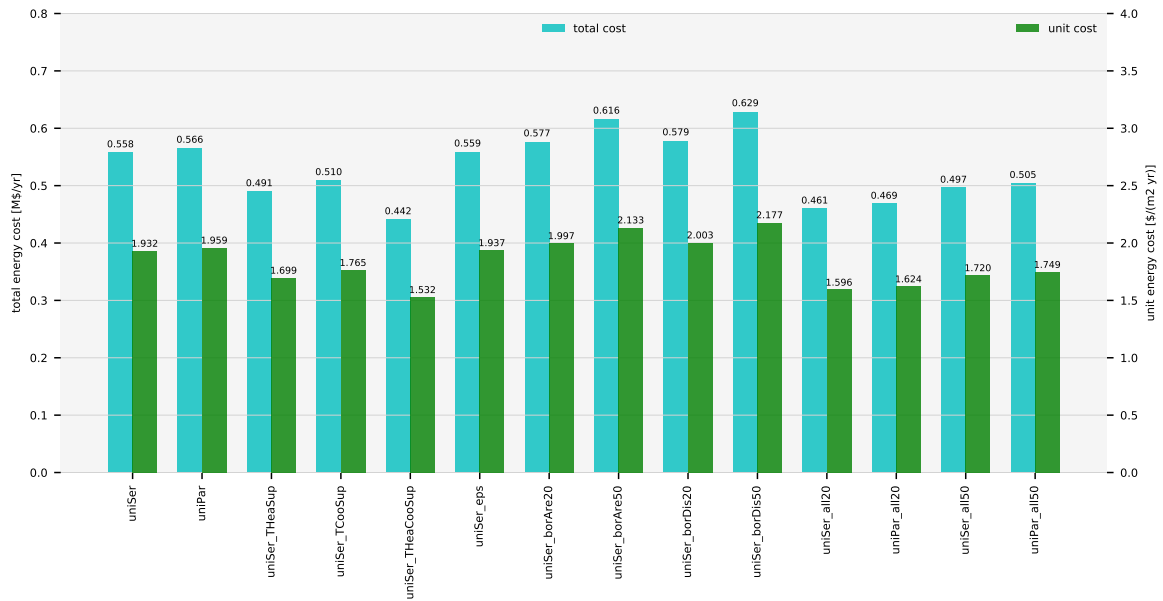


Fig. 6.6: Annual energy costs for all simulated cases. Auxiliary heat added at the central plant was assumed to be supplied by an air to water heat pump with $COP_h = 2.5$.

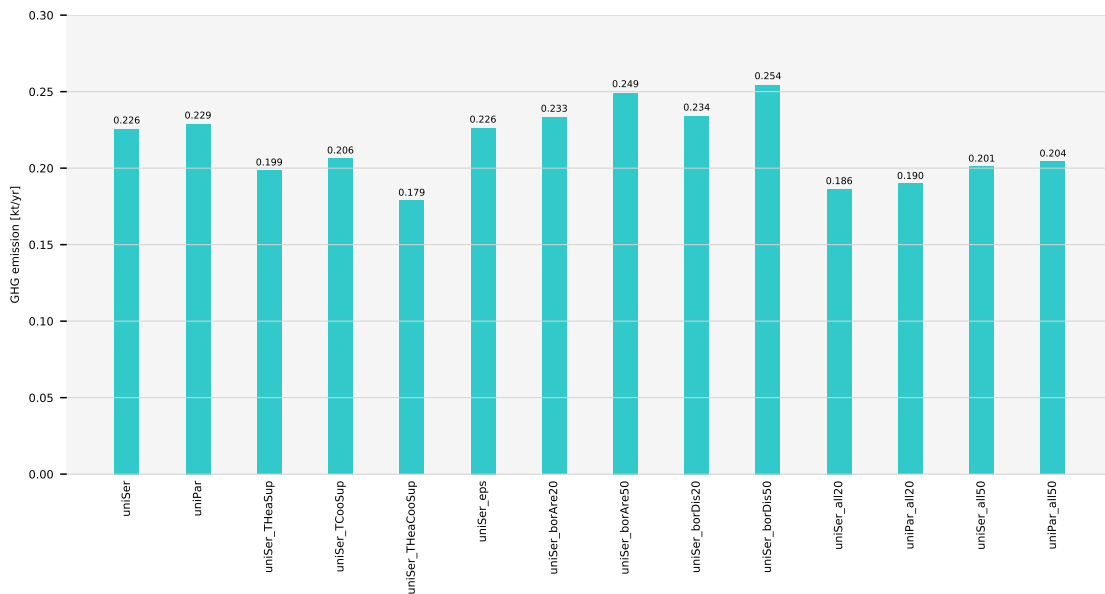


Fig. 6.7: Annual greenhouse gas emission for all simulated cases. Auxiliary heat added at the central plant was assumed to be supplied by an air to water heat pump with $COP_h = 2.5$.

Fig. 6.4, Fig. 6.5, Fig. 6.6 and Fig. 6.7 compare the energy break-down, energy use, energy costs and GHG emissions for all simulated cases. It turns out that the series configuration lead to 1.4% less energy use and 1.3% less GHG emissions than the parallel configuration. We therefore recommend to use the series configuration, which is also easier to extend and control. The biggest energy savings are achieved if the design water temperature for space heating is reduced from 41°C to 30°C, and the design water temperature for space cooling is raised from 4°C to 10°C. The energy savings are 12.0% for a decrease in heating temperature, 8.6% for a raise in cooling temperature, and 20.7% for the combined change in heating and cooling temperatures. Increasing the heat exchanger effectiveness from 71% to 90% has no noticeable effect. Reducing the number of boreholes, either by reducing the overall area by 20% or by increasing the spacing between the drillings by a factor of $1/\sqrt{0.8}$, increases energy consumption by 3.4%. When either reducing the overall area by half or increasing the spacing by a factor of $1/\sqrt{0.5}$, energy consumption increases by 12.7%. Hence, a moderate reduction of the number of boreholes could be an effective measure to reduce costs.

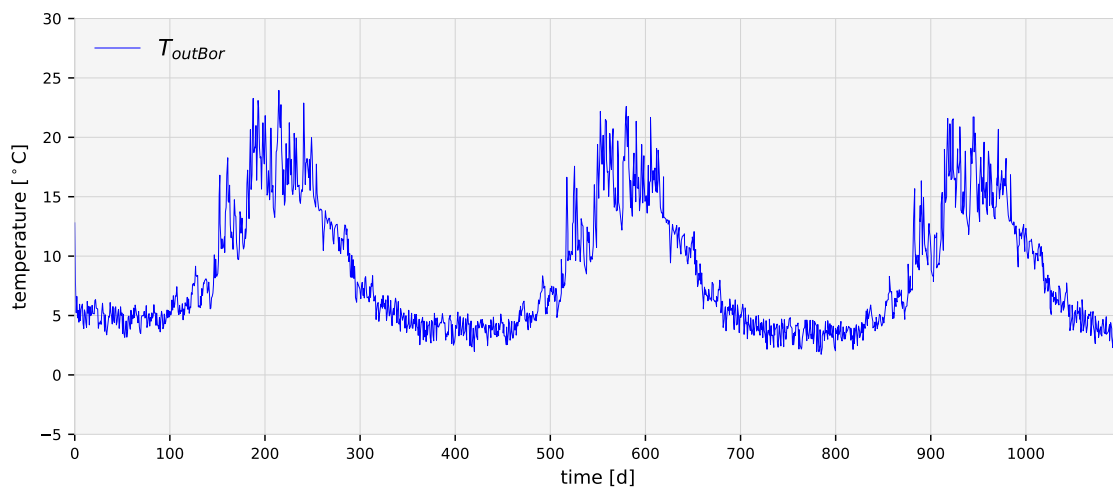


Fig. 6.8: Borefield outlet water temperatures over 3 years operation for the case uniSer_all20 in Table 6.1. The temperature remains similar over the 3 years.

6.3 Analysis of the latest design change

To reduce the cost of the geothermal fields, the design team proposed the following change: Instead of the system shown in Fig. 5.6 which has between borefield and load only a heat pump but no heat exchangers, the new system is as shown in Fig. 6.9. In the new system, the geothermal field is no longer part of the substation, but rather connected to the return pipe of the district heating and cooling system. Moreover, it is operated with glycol with a return temperature of about -1°C in heating operation. A heat pump boosts this temperature up to a district loop temperature of about 8°C to 12°C in heating mode. In cooling mode, this heat pump is by-passed with a glycol-to-water heat exchanger. The heat pump and the heat exchanger are connected in series into the district return pipe.

Furthermore, the substation hydraulic changed: It now uses a multi-stack heat pump, connected directly to the distribution loop with a control valve. On the load side of the multi-stack heat pump, there is a heat exchanger between multi-stack heat pump and heating load, and between multi-stack heat pump and cooling load.

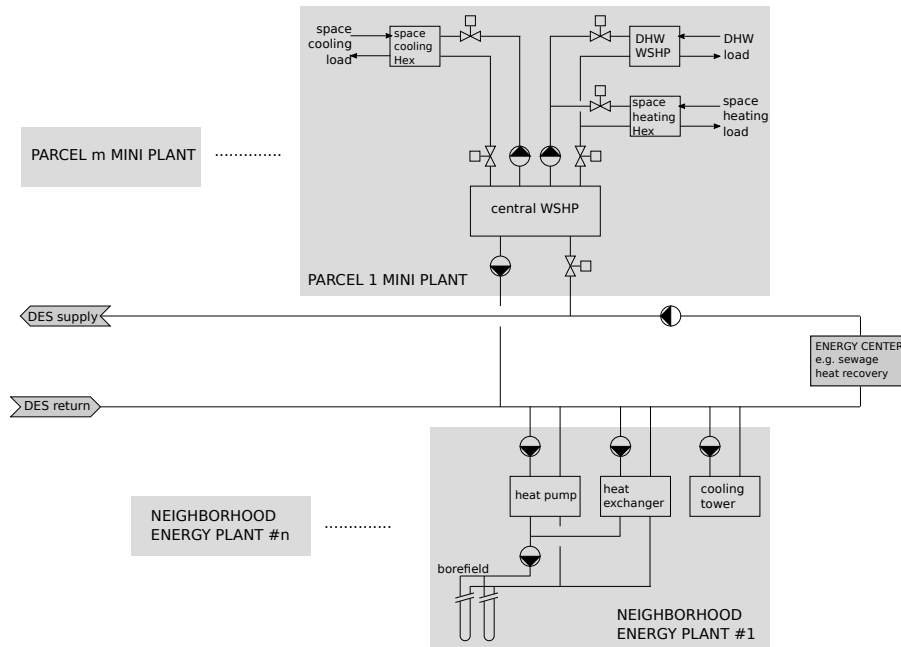


Fig. 6.9: Latest system schematic, used in the analysis of Section 6.3.

6.3.1 Efficiency penalty

To estimate how the compressor energy changes due to the new design, we conducted a high-level analysis based on the 2nd law of thermodynamics. This analysis, which is described below, is based on the change in heat pump COP, estimated as

$$COP_h = \frac{Q_h}{P} = \eta \frac{T_h}{T_h - T_c}, \quad (6.1)$$

where Q_h is the useful heat, P is the compressor energy, η is the efficiency of how close the actual COP is compared to the Carnot efficiency, and T_h and T_c are the hot and cold side temperatures. To compute the change in efficiency between the original and the new design, we compute the efficiency penalty f which we define as

$$f = \frac{P_2}{P_1} = \frac{T_{h,2} - T_{c,2}}{T_{h,1} - T_{c,1}}, \quad (6.2)$$

where the subscripts 1 and 2 are the original and new design.

6.3.1.1 Efficiency penalty due to lower borefield temperature during heating

In heating conditions, the leaving glycol temperature from the geothermal field is in our simulated system around 7°C (see T_{outBor} in Fig. 6.1), while it is in the new design around -1°C . Assuming a temperature of the heating load of 35°C , the resulting increase in compressor energy is

$$f_{h,1} = \frac{T_{h,2} - T_{c,2}}{T_{h,1} - T_{c,1}} = \frac{35 - (-1)}{35 - 7} = 1.29. \quad (6.3)$$

Hence, compressor energy increases by about 30%.

6.3.1.2 Efficiency penalty due to additional heat exchangers during heating

The original design shown in Fig. 5.6 has between borefield and load only a heat pump but no heat exchangers. The new design has two heat pumps plus one heat exchanger (assuming the borefield heat exchanger is bypassed) between the borefield and the heating load. Assuming a 2 Kelvin approach temperature at the load-side heat exchanger, and a 1 Kelvin approach temperature at each, the evaporator and condenser of the glycol-water heat pump, the additional temperature lift of this configuration is $\Delta T_{app,tot} = 4$ Kelvin. Assuming a total temperature lift between borefield and heating load of 35 Kelvin, this further increases the compressor energy by

$$f_{h,2} = \frac{(T_h - T_c) + \Delta T_{app,tot}}{T_h - T_c} = \frac{35 + 4}{35} = 1.11. \quad (6.4)$$

Hence, the heat exchangers increase the compressor energy by an additional 10%.

6.3.1.3 Total efficiency penalty during heating

The two effects are multiplicative. Hence, the total efficiency penalty is

$$f_h = f_{h,1} f_{h,2} = 1.29 \cdot 1.11 = 1.43, \quad (6.5)$$

or about 43%. The electricity costs are about \$558 k/a (see Fig. 6.6), of which about 75% is for compressor (see Fig. 6.5), this results in \$180 k/a ($= 0.43 \cdot 558 \cdot 0.75$) higher electricity costs.

Assuming about 0.226 kt/a GHG emissions (see Fig. 6.7), the increase would be about 0.07 kt/a ($= 0.43 \cdot 0.226 \cdot 0.75$).

6.3.1.4 Efficiency penalty due to additional heat exchangers during geothermal cooling

As described above, the original design shown in Fig. 5.6 has between borefield and load only a heat pump but no heat exchangers. The new design has in cooling mode an additional two heat exchangers between borefield and cooling load. Assuming again an approach temperature of $\Delta T_{app} = 2$ Kelvin for each of the two heat exchangers, a leaving glycol temperature from the borefield of 20°C and a cooling load temperature of 10°C, the efficiency penalty for the new design is

$$f_{c,hex} = \frac{(T_h - T_c) + \Delta T_{app,tot}}{T_h - T_c} = \frac{10 + 4}{10} = 1.4, \quad (6.6)$$

or about 40%.

6.3.1.5 Efficiency penalty due to additional heat exchangers in heat recovery mode

In the heat recovery mode, the original design shown in Fig. 5.6 has only a heat pump (and two buffer tanks that won't affect the temperature lift) whereas the new design has an additional two heat exchangers. Assuming again a heating load temperature of 35°C, a cooling load temperature of 10°C and an approach temperature of $\Delta T_{app} = 2$ Kelvin for each of the two heat exchangers, the efficiency penalty for the new design is

$$f_{c,hr} = \frac{(T_h - T_c) + \Delta T_{app,tot}}{T_h - T_c} = \frac{(35 - 10) + 4}{35 - 10} = 1.16, \quad (6.7)$$

or about 15%.

6.3.2 Comments on controllability and extensibility

The recent change makes the control of the energy transfer station more complex. For example, there are four cascading control loops formed through the valve of the load-side heat exchanger, the multi-stage heat pump, the substation valve and pump and the central district pump. These control loops will be harder to tune than the control of the system shown in Fig. 5.6.

Furthermore, the simulations show no difference in energy use between the series and the parallel connection of the substations. A concept for how to modularly extend the district loop and how to connect higher temperature waste heat is discussed in Section 4.3. As this is a strength of the series connection, and has not yet been shown for the parallel configuration, we recommend to use the series configuration.

6.3.3 Summary on design changes

The new design leads to a more complex hydraulic and to cascading control loops. Both make it harder to operate the system at its peak performance and ensure its efficiency during its lifetime.

Moreover, the new design is less efficient. Compressor energy is expected to increase, compared to the original design shown in Fig. 5.6 as follows:

- 43% for geothermal heating,
- 40% for geothermal cooling, and
- 16% for heat recovery mode.

As there seems to be little load diversity within each building, and the buildings have no buffer storage tank, we estimate that the dominant energy use is for geothermal heating and cooling combined. Thus, assuming a 40% higher compressor energy results in about \$180 k/a higher electricity costs and about 0.07 kt/a higher GHG emissions.

Therefore, all other things being equal, the design shown in Fig. 5.6 seems superior.

Chapter 7

Bibliography

- [Tor18] *Annual Energy Consumption & Greenhouse Gas (GHG) Emissions*. July 2018. URL: <https://www.toronto.ca/legdocs/mmis/2018/pe/bgrd/backgroundfile-117753.pdf>.
- [BunningWFMuller18] Felix Bünning, Michael Wetter, Marcus Fuchs, and Dirk Müller. Bidirectional low temperature district energy systems with agent-based control: performance comparison and operation optimization. *Applied Energy*, 209:502–515, 2018. URL: <https://doi.org/10.1016/j.apenergy.2017.10.072>, doi:DOI:10.1016/j.apenergy.2017.10.072.
- [Gau15] Thomas Gautschi. *Anergienetze in Betrieb*. Technical Report 66, Amstein + Walthert AG, 2015. URL: http://www.lsta.lt/files/events/2016-04-18_EHPkonfer/Pranesimai/Stadtekongress/T.Gautschi.pdf.
- [ME97] Sven Erik Mattsson and Hilding Elmqvist. Modelica – An international effort to design the next generation modeling language. In L. Boullart, M. Loccupier, and Sven Erik Mattsson, editors, *7th IFAC Symposium on Computer Aided Control Systems Design*, 1–5. Gent, Belgium, April 1997. URL: <http://www.modelica.org/publications/papers/CACSD97Modelica.pdf>.
- [SKrauchiS15] Thomas Schluck, Philipp Kräuchi, and Matthias Sulzer. Non-linear thermal networks - how can a meshed network improve energy efficiency? In *Proceedings of International Conference CISBAT*, 779–785. Lausanne, Switzerland, September 2015. doi:10.5075/epfl-cisbat2015-779-784.
- [Sul18] Matthias Sulzer. Private communication with Michael Wetter, August 2018.
- [SSS18] Matthias Sulzer, Artem Sotnikov, and Tobias Sommer. Reservoir-Niedertemperatur Netztopologie für die Vermaschung von thermischen Netzen. In *Status-Seminar Forschen für den Bau im Kontext von Energie und Umwelt*. Zürich, Switzerland, September 2018. ETH Zürich.
- [VS15] Nadège Vetterli and Matthias Sulzer. Dynamic analysis of the low-temperature district network “Suurstoffi” through monitoring. In *Proceedings of International Conference CISBAT 2015 Future Buildings and Districts Sustainability from Nano to Urban Scale*, number EPFL-CONF-213373, 517–522. LESO-PB, EPFL, 2015.
- [WZNP14] Michael Wetter, Wangda Zuo, Thierry S. Noudui, and Xiufeng Pang. Modelica Buildings library. *Journal of Building Performance Simulation*, 7(4):253–270, 2014. doi:DOI:10.1080/19401493.2013.765506.

-
- [WM08] S. Wilcox and W. Marion. Users manual for TMY3 data sets. Technical Report NREL/TP-581-43156, NREL, Golden, CO, May 2008.
-